Available online at www.sciencedirect.com

SciVerse ScienceDirect

Ceramics International 39 (2013) 2981–2987

CERAMICS INTERNATIONAL

www.elsevier.com/locate/ceramint

Photo-catalytic efficiency of laboratory made and commercially available ceramic building products

Vilma Ducman[a,*], Vladimira Petrovič[a], Srečo D. Škapin[b]

[a]*Slovenian National Building and Civil Engineering Institute, Dimičeva 12, 1000 Ljubljana, Slovenia*
[b]*Jožef Stefan Institute, Jamova 39, 1000 Ljubljana, Slovenia*

Received 10 July 2012; received in revised form 21 September 2012; accepted 24 September 2012
Available online 3 October 2012

Abstract

Self-cleaning building products are mainly based on the application of nanotitania onto exposed outdoor surfaces. In order to achieve high self-cleaning efficiency for outdoor applications, it is important that nanotitania is in the form of anatase, and that particle sizes (also in the case of additional thermal treatment) are in the nano-range, so that a large enough specific surface area can be activated. The particle size and the mineralogy of the photocatalytic layers were determined by means of SEM and Raman spectroscopy, respectively.

The self-cleaning efficiency of nanotitania-based material can be evaluated by different methods; in the present paper the suitability of the method based on the discolouration of methylene blue was verified on some samples that were prepared in-lab (through the application of commercially available TiO_2 sol onto a ceramic substrate), as well as on samples of commercially available products.

Keywords: Photo-catalysis; TiO_2; MB discolouration; Raman spectroscopy

1. Introduction

The surfaces of exposed building materials, such as ceramic tiles, roofing tiles, glass, and facades, are exposed to environmental conditions which can result in the depositing of dirt onto them, so that cleaning, which is connected to a high consumption of energy, labor, and detergents, is needed, resulting in high maintenance costs.

In order to reduce costs and improve the long-term esthetic appearance of the exposed surfaces of building materials, nano-TiO_2 coatings, with photocatalytic and hydrophilic properties, can be applied. If TiO_2 is illuminated by UV light, grease and other dirt of organic origin decompose, and when the TiO_2 surface becomes super-hydrophilic, its high affinity for water results in a self-cleaning effect, as rainwater can remove dirt from the surface due to its preferential adsorption [1]. The initial process of photocatalysis consists of the generation of charged carriers, electrons and holes, after the absorption of efficient photon energy ($h\nu \geq E_g = 3.2$ eV) by titania; e^- are the electrons in the conduction band and h^+ are the electron vacancy in the valence band of a semiconductor like TiO_2.

$$TiO_2 + h\nu \rightarrow TiO_2 + h^+ + e^- \quad (1)$$

The separated e^- and h^+ can recombine in bulk or on the particle surface forming $e^- - h^+$ pairs, and causing deactivation of the photocatalytic reaction.

If charge separation is maintained, the e^- and h^+ can migrate to the surface of the TiO_2 particles, where they participate in reactions with adsorbed water and oxygen to form reactive radicals. The latter then react with organic molecules and dirt; the e^- participate in a reaction with an oxidant, i.e. acceptor molecule (oxygen from the air) in order to produce a reduced product (the super-oxide ions $O_2^{\bullet -}$, which are also highly reactive and are able to oxidize organic materials);

$$(O_2)_{ads} + e^- \rightarrow O_2^{\bullet -} \quad (2)$$

*Corresponding author.
E-mail address: vilma.ducman@zag.si (V. Ducman).
URLS: http://www.zag.si (V. Ducman), http://www.zag.si (V. Petrovič), http://www.ijs.si (S.D. Škapin).

0272-8842/$ - see front matter © 2012 Elsevier Ltd and Techna Group S.r.l. All rights reserved.
http://dx.doi.org/10.1016/j.ceramint.2012.09.075

The h^+ (holes) participate in the reaction with the adsorbed donor (water) to produce an oxidized product (the highly reactive hydroxyl radical (•OH));

$$(H_2O \leftrightarrow H^+ + OH^-)_{ads} + h^+ \rightarrow \bullet OH + H^+ \quad (3)$$

Both the super-oxide ions and the hydroxyl radicals then proceed to oxidize the adsorbed organic molecules. In this way, for example, grease and oils can be fully mineralized into carbon dioxide and water [2].

The application of photocatalysts to building products began in the early 1990s. Building products which can be presently upgraded by photocatalytical coatings include: ceramic tiles, glass, panels, soundproofing walls, tunnel walls, road blocks and concrete pavements [3].

Nanotitania can be deposited by different techniques with regard to the final product and its use (e.g. the spray technique, inkjet printing) [4], and is frequently additionally subjected to a high temperature process up to 900 °C in order to improve its adhesion properties [5–7]. Such thermal treatment can significantly influence its photocatalytic efficiency, affecting its two most important parameters. Firstly, if the temperature of fixing is too high, the anatase transforms into rutile which is much less photocatalytically active for outdoor applications (under UV illumination). Secondly, during the heating process, the particles of nanotitania start to grow, which causes a lowering in their specific surface area, and consequently reduces photo-catalytic efficiency [8].

Numerous experimental methods have been developed for the evaluation of the photocatalytic efficiency of the three different phase systems: the gas–solid phase system, the liquid–solid phase system and the solid–solid phase system. Much progress was made in this field by the International Organization for Standardization under technical commitee TC 206 Fine ceramics, which, from 2007 onwards, has published 7 new standards on photocatalytic efficiency [9–15]. Some other such standards are still being developed. Efforts have also been made through the COST 540 action [16] to develop specific methods with high sensitivity; e.g. the decomposition of isopropanol into acetone and further into water and CO_2 [17], or the degradation of terephthalic acid into hydroxyterephthalic acid, which is highly fluorescent and as such can be easily detected by means of HPLC-FLD [18].

Of all the methods, discolouration of methylene blue (MB) dye as a model pollutant is most often used for the testing of materials with self-cleaning properties [9,19–23]. It is based on the monitoring of the discolouration (decomposition) of the MB in de-ionized water when the solution is in contact with the photocatalyst (i.e. a liquid–solid system).

The goal of the work presented in this paper was to prepare photocatalytic samples in the laboratory, and to compare the properties of the nanotitania coatings, after performance of the firing process, with regard to size, mineralogical phase and self-cleaning efficiency, with those of selected commercially available photocatalytic products.

2. Experimental

2.1. Materials and preparation

Ceramic tile samples with titania coatings were prepared in the laboratory from TiO_2 suspensions (1% and 4%) in isopropanol based on Hombikat XXS 100 (Sachtleben Chemie GmbH) sol of anatase of declared size 7 nm. The suspensions were stirred for 24 h at room temperature and then deposited on the ceramic tiles, which had smooth surfaces, by means of a spray technique, at a pressure of 6 bars. The titania films were dried at 100 °C for 30 min, and then fired up to 700 °C and 850 °C at a rate of 100 °C/h, using a dwelling time of 30 min at the selected temperature.

The investigated commercially available samples of ceramic tiles, glass and roofing tiles which were declared to be photo-catalytically efficient were obtained directly from the market.

2.2. Characterization of the samples

The morphology and particle size of the nanotitania coatings were determined by Field Emission-Scanning Electron Microscopy (FE-SEM), using a Supra 35 VP, Carl Zeiss electron microscope. Particle size was determined from SEM micrographs using Image Tool for Windows software (version 2.0).

Raman spectra were recorded in order to determine the mineralogical phase (anataze/rutile) using a LabRam HR800 Raman spectrometer (HORIBA Jobin Yvone) equipped with an Olympus BXFM optical microscope and an air-cooled CCD detector. The samples were excited by the 514.45 nm line of an Argon ion laser operating at a power of 17 mW, using neutral density filters.

2.3. Performance of the photo-catalytic tests

The samples were first pre-irradiated in an irradiation chamber equipped with two parallel UV-A bulbs (40 W, Osram Eversun, $\lambda_{max} = 360$ nm, 10.0 W/m^2) in order to decompose any possibly remaining organic contaminants by photo-catalytic oxidation. A cylindrically shaped glass cell, with an inner diameter of 40 mm, was attached to each sample using silicon glue. Since the substrates tend to adsorb the dye molecules, pre-adsorption of the surface was performed using a 20 μmol/L aqueous methylene blue solution. After the adsorption process of the dye was complete, the adsorption solution was replaced by 40 ml of the test solution (10 μmol/L) and the samples were exposed to UV-A light in the irradiation chamber using Osram Eversun bulbs (40 W, $\lambda_{max} = 360$ nm, 10.0 W/m2). The decomposition rate of the dye under the UV-A light irradiation was determined by measuring its maximum absorption spectrum at 664 nm using a UV/VIS spectrophotometer (Ocean Optics Inc.) every 2 h. The photo-catalytic activity of the TiO_2 was defined as the photo-degradation rate of the dye (i.e. the rate of decrease

of the dye concentration), and calculated using the following equation [24]:

$$\text{Photo-degradation efficiency } (\eta) = \frac{A_0 - A_t}{A_0} 100\% \quad (4)$$

where A_0 is the initial absorption of the dye, and A_t is the absorption of the dye at a given UV irradiation time.

In order to assess the photocatalytic efficiency of the TiO_2 coated samples, measurements were also performed on inert laboratory glass, which was designated as a "blank" sample.

3. Results

The samples that were prepared in the laboratory, as well as those taken from the market, were analyzed with regard to the morphology of the nanotitania coatings and the presence of the mineralogical form of anatase. Their photocatalytic efficiency was determined by means of methylene blue discolouration.

3.1. Morphology

The laboratory prepared samples with 1% and 4% of TiO_2 suspensions were analyzed by SEM after drying at 100 °C, and firing at 700 °C and 850 °C. As can be seen in Figs. 1 and 2, after heat treatment the TiO_2 particles remained within the sub-micron size range; drying at 100 °C had no influence on the particle size and morphology (Fig. 1a and Fig. 2a). However, when the samples were heated to 700 °C the particles grew in size due to coalescence. Partially connected particles with a size of 25 nm formed the porous surface of a nanotitania layer where some cracks could be identified (Fig. 1c). According to the particle morphology and Raman spectroscopy, the particles crystallized in an anatase modification.

Upon heating to a temperature of 850 °C, the TiO_2 particles appeared in two morphologies, as spherically and rod-shaped particles. The spherically-shaped particles had the same size range, i.e. about 35 nm, as the anatase particles that were fired at 700 °C. Additionally, the rod-shaped particles had the shape of a nearly rectangular parallelepiped, with a width of approximately 80 nm and lengths up to 500 nm, although length is difficult to measure accurately since one end of these particles is usually merged into the TiO_2 layer (Fig. 1c and Fig. 2c). Elongated particle morphology is typical for rutile modification.

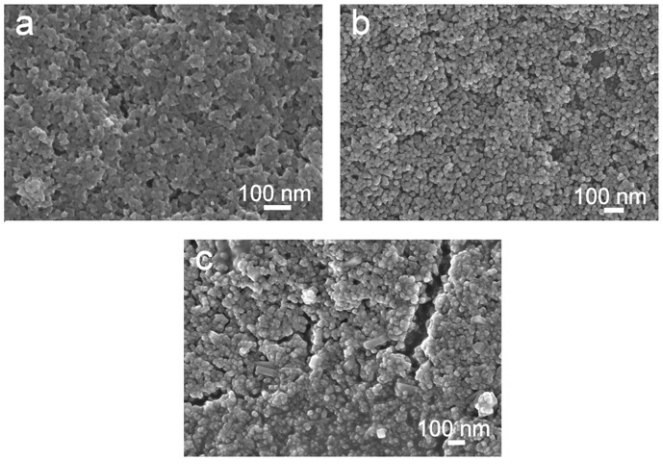

Fig. 1. SEM images of (a) a laboratory prepared sample with 1% TiO_2 dried at 100 °C, (b) the same sample after firing at 700 °C, and (c) after firing at 850 °C.

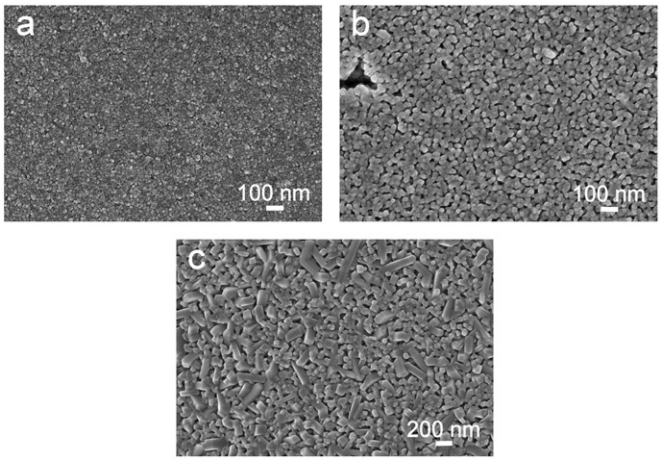

Fig. 2. SEM images of (a) a laboratory prepared sample with 4% TiO_2 dried at 100 °C, (b) the same sample after firing at 700 °C, and (c) after firing at 850 °C.

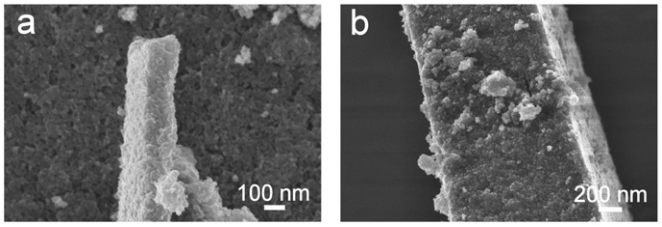

Fig. 3. The thickness of the titania layer in the case of application of (a) a 1% and (b) a 4% solution of nanotitania, and after drying at 100 °C.

The sample prepared from the 1% nanotitania solution had a thinner layer of TiO_2 than the samples prepared from the 4% solution. The thicknesses of the TiO_2 layer were determined by means of SEM, which was performed on the previously scratched surface (Fig. 3a and b). In the case of the application of the 1% solution, the layer thickness was in the order of 100 nm, whereas, in the case of the 4% solution it amounted to one micron. When comparing Fig. 1c and Fig. 2c, which represent samples with 1% and 4% of nanotitania, it can be observed that in the case of the 1% nanotitania solution, and after firing at 850 °C, a glaze covered some parts of the titania layer (Fig. 1c). However no traces of such a glaze was observed in the case of the application of a 4% nanotitania solution (Fig. 2c), which can be attributed to the much greater thickness of the nanotitania layer.

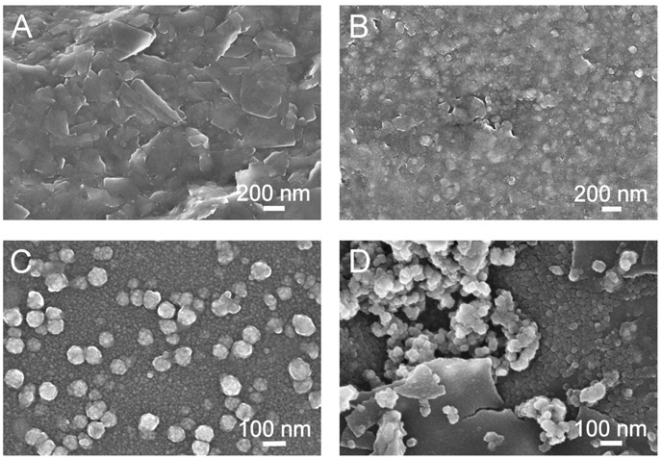

Fig. 4. SEM images of four different commercial samples: self-cleaning ceramic tiles (A, B), self-cleaning glass (C), and a self-cleaning clay roof tile (D).

Investigation of the commercial samples also confirmed the presence of nano-sized particles on their surfaces (Fig. 4). The grains can be most easily distinguished on the glass surfaces. On other surfaces, especially on the ceramic tiles (samples A and B) it appears that the particles of nanotitania are partially covered by a glaze.

3.2. Mineralogical composition of the titania coatings

The mineralogical composition of the nanotitania coating was determined by means of Raman spectroscopy. In Fig. 5 it can be seen that, in the case of the laboratory prepared samples, after drying at 100 °C and firing at 700 °C (Fig. 5a and b), TiO_2 in the form of anatase is present. The Raman spectrum of a single anatase crystal has been investigated by Ohsaka et al. [25], who concluded that anatase has six Raman active modes, which appear at 144 cm^{-1} (E_g), 197 cm^{-1} (E_g), 399 cm^{-1} (B_{1g}), 513 cm^{-1} (A_{1g}), 519 cm^{-1} (B_{1g}), and 639 cm^{-1} (E_g). In our study the observed band positions were in agreement with the results of previous reports for the anatase phase, and the characteristic peaks for anatase were 150 cm^{-1}(E_g), 403 cm^{-1}(B_{1g}), 516 cm^{-1}(A_{1g}) and 640 cm^{-1} (E_g) (Fig. 5a) and 143 cm^{-1} (E_g), 197 cm^{-1} (E_g), 396 cm^{-1}(B_{1g}), 518 cm^{-1}(B_{1g}) and 640 cm^{-1}(E_g) (Fig. 5b). In the Raman spectrum of anatase from the laboratory prepared samples, the observed broadening and shifts of the Raman peaks/bands are due to the effects of different particle sizes and the vibrational amplitudes of the nearest neighbor bonds. After firing at 850 °C, the nanotitania was present in the rutile phase, as well as anatase, with characteristic peaks at 144 cm^{-1} (B_{1g}), 235 cm^{-1} (2 phonon process), 446 cm^{-1}(E_g), and 615 cm^{-1} (A_{1g}), which are assigned to rutile, and at 197 cm^{-1} (E_g), 398 cm^{-1}(B_{1g}), 516 cm^{-1} (A_{1g}) and 640 cm^{-1} (E_g) which have been assigned to anatase (Fig. 5c) [26].

Investigation of the commercially available building products also confirmed the presence of anatase in all

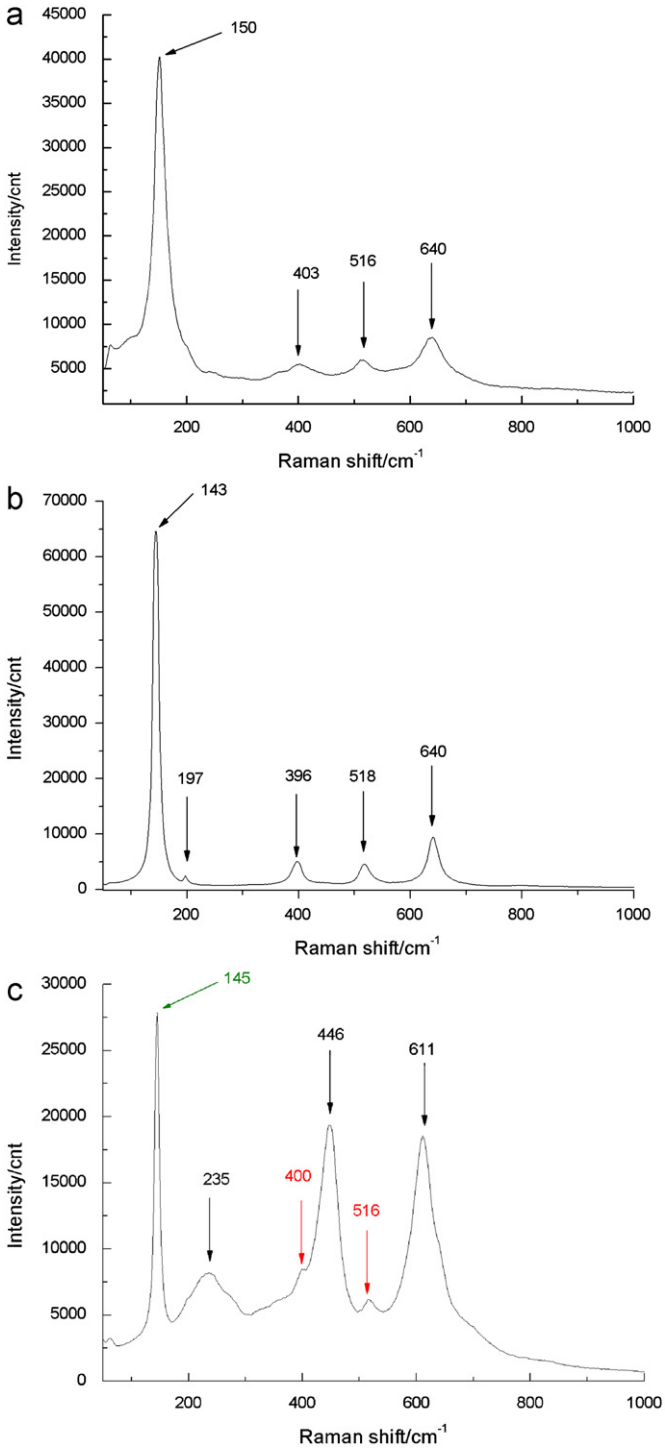

Fig. 5. Raman spectra of the laboratory-prepared sample with TiO_2, dried at 100 °C (a), and fired at 700 °C (b) and 850 °C (c). The characteristic peaks for anatase are marked by dash-dotted arrows, and those corresponding to rutile by solid arrows. Experimental conditions: λ_{ex}= 514.45 nm.

cases (Fig. 6), even though in the case of self-cleaning glass (sample C) the peaks were not easily distinguishable, except for the peak at 145 cm^{-1}. In the case of both ceramic tiles (A, B), the presence of zircon ($ZrSiO_4$), too, is evident. Zircon is widely employed in glazes as an effective and inexpensive opacifier [27]. The spectrum of zircon

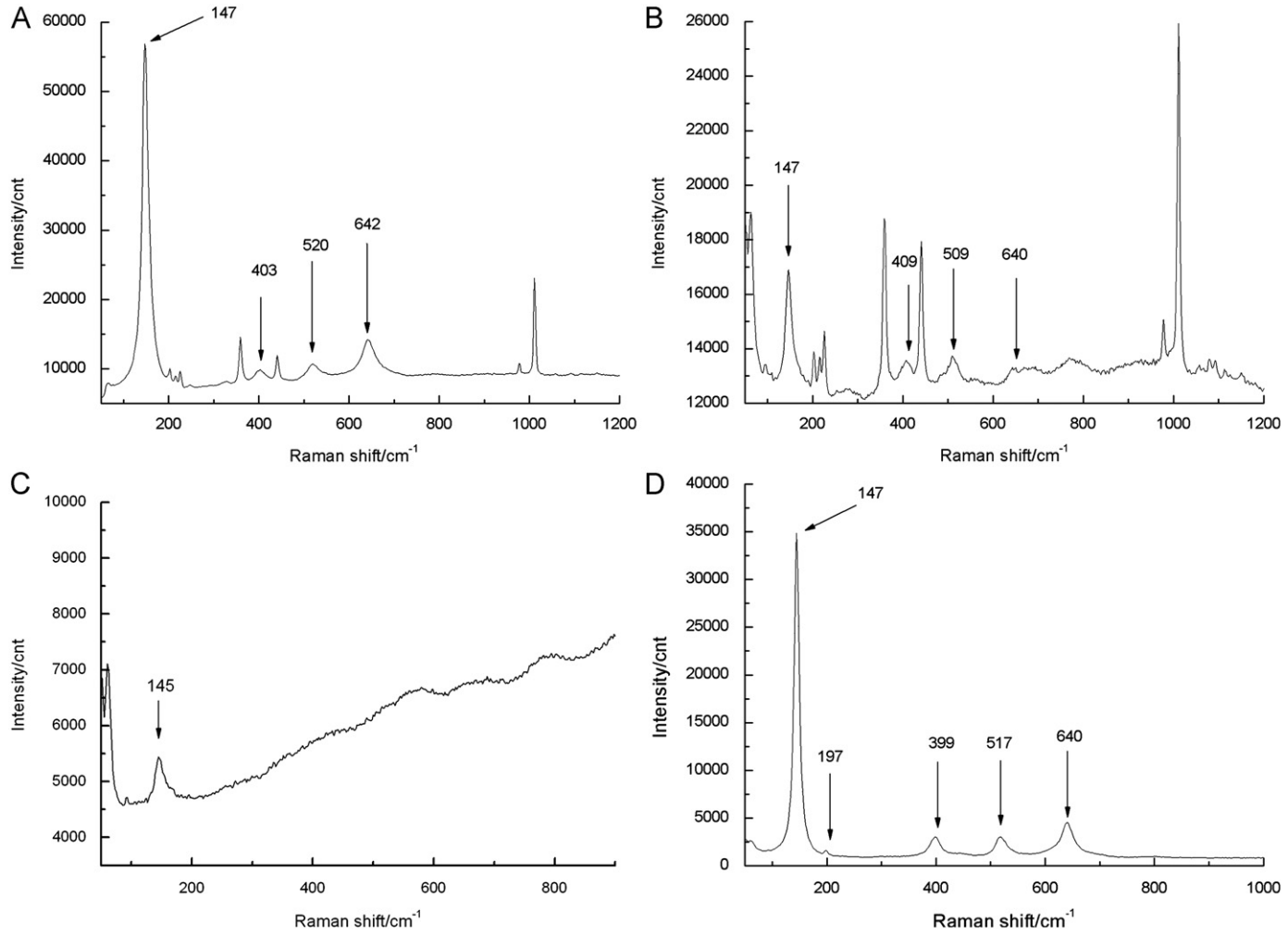

Fig. 6. Raman spectra of the commercial samples: self-cleaning ceramic tiles (A, B), self-cleaning glass (C), and a self-cleaning clay roof tile (D). The characteristic peaks for anatase are marked by arrows. Experimental conditions: $\lambda_{ex} =$ 514.45 nm.

exhibits strong bands near 1008 cm^{-1} and near 974 cm^{-1}. Other relatively strong Raman bands corresponding to zircon are located in the low frequency part, at 439, 357, 225, 202, 214 and 393 cm^{-1} [28].

3.3. Photocatalytic efficiency

Two laboratory prepared samples and four selected commercial self-cleaning building products were exposed to UV light, and decomposition of the methylene blue dye was monitored by means of an UV/VIS spectrophotometer. The results for the laboratory samples are presented in Figs. 7 and 8, the results corresponding to the commercial self-cleaning building products are given in Fig. 9.

The results for the laboratory prepared samples, the first one after drying at 100 °C, and for the second one after firing at 700 °C, confirmed that they are highly efficient; even though degradation was somewhat lower after firing at 700 °C. The degradation of methylene blue was greater than 60% after exposure to UV for 6 h in both cases. Efficiency after firing at 850 °C was, as expected,

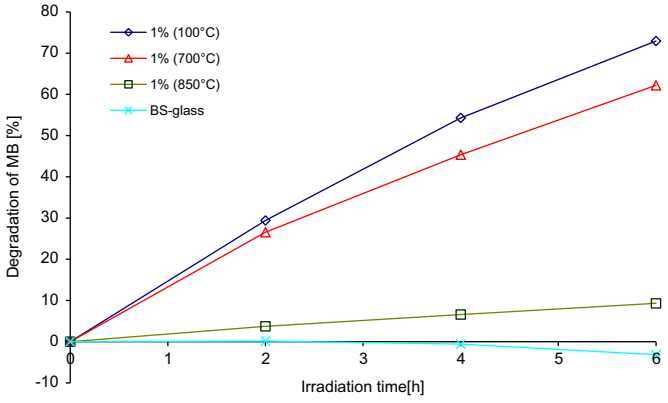

Fig. 7. Photo-degradation of MB as a function of irradiation time for the laboratory prepared sample with 1% TiO_2, dried at 100 °C, and heated to 700 °C and 850 °C. Light intensity: 10.0 W/m^2.

significantly lower; after 6 h of exposure the decomposition of methylene blue was 16%. This drop in efficiency is a result of the partial phase transformation of anatase into

rutile (Fig. 4c). It is well known that the rutile phase is not so efficient under UV light [29]. This not insignificant drop in photocatalytic efficiency was due to the growth of titania grains (Fig. 1c and Fig. 2c) [8,30], as well as to the melted glaze which covered the titania film. Due to these phenomena, the titania particles were protected from the effects of UV light, which cannot reach the active sides of the photocatalyst.

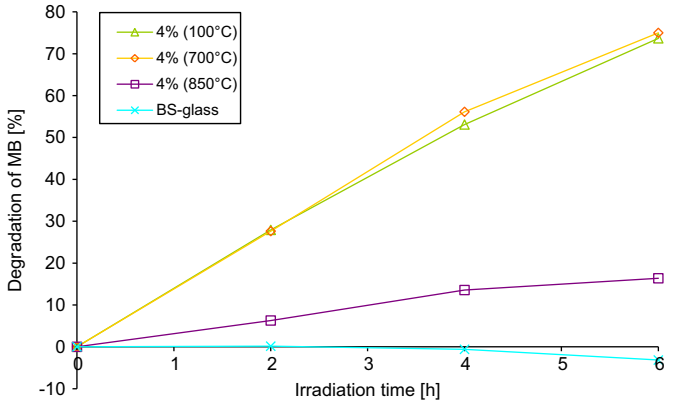

Fig. 8. Photo-degradation of MB as a function of irradiation time for the laboratory prepared sample with 4% TiO_2, dried at 100 °C, and heated to 700 °C and 850 °C. Light intensity: 10.0 W/m^2.

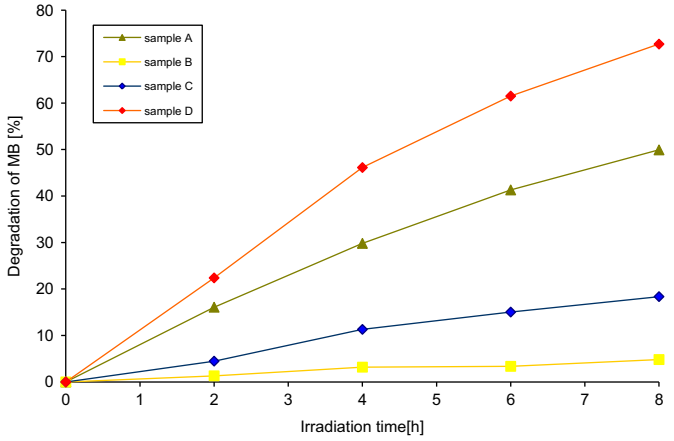

Fig. 9. Photo-degradation of MB as a function of irradiation time for the investigated commercially available self-cleaning products: self-cleaning ceramic tiles (A, B), self-cleaning glass (C), and a self-cleaning clay roof tile (D). Light intensity: 10 W/m^2.

All the commercially available products also showed photo-catalytic activity. A summary of the photo-catalytic efficiency of the commercially available and laboratory prepared samples, after 2 and 6 h of exposure, is given in Table 1.

Comparing the different commercial products, it can be seen that ceramic tile A is much more effective then ceramic tile B; in both cases anatase is present as the mineral phase of titania, and in both cases the particles are within the nanosize range. But SEM analysis showed that, in the case of tile B, there is a shiny hue on the surface which could be ascribed to a very thin layer of glaze over the nanotitania. Such a very thin layer of glaze does not influence Raman detection (Fig. 6b), but could hinder photo-induced activity (Fig. 9, sample B).

4. Conclusions

Laboratory prepared samples and samples of commercially available products were analyzed with regard to the presence of the titania mineral phase anatase, the particle size of the titania, and its photocatalytic activity, as measured by the decomposition of the methylene blue dye. The results of Raman spectroscopy confirmed the presence of the mineral phase anatase in all the samples which exhibited photocatalytic efficiency, which proves that this technique is valuable as a fast-tracking qualitative method which can be used to determine mineralogical composition; in this case, anatase. The results of the SEM investigations confirmed the presence of nano-sized grains of TiO_2 in all the efficient coatings, where the particles had sizes significantly less than 100 nm. After the coatings had been fired up to 850 °C, the titania grains increased in size, and a transformation from the anatase to the rutile form took place, which resulted in the occurrence of rod-shaped particles with lengths of up to 500 nm. The differences which were observed in the efficiency of the coatings can be mainly ascribed to the different amounts of titania which

Table 1
The photocatalytic efficiency of the commercially available and laboratory prepared samples after 2 and 6 h of exposure to UV radiation.

Sample	Decomposition of MB after 2 h (%)	Decomposition of MB after 6 h (%)
Ceramic tile A	16	41
Ceramic tile B	1	3
Glass C	4	15
Roofing tile D	22	62
Laboratory sample with 1% TiO_2—dried at 100 °C	29	73
Laboratory sample with 1% TiO_2—fired at 700 °C	31	61
Laboratory sample with 1% TiO_2—fired at 850 °C	4	9
Laboratory sample with 4% TiO_2—dried at 100 °C	28	74
Laboratory sample with 4% TiO_2—fired at 700 °C	28	75
Laboratory sample with 4% TiO_2—fired at 850 °C	6	16

the coatings contained, the (partial) transformation of anatase into rutile, and the occurrence of grain growth.

A combination of all three methods: SEM, Raman spectroscopy, and the methylene blue discolouration method can thus provide a valuable insight into relevant parameters of the photo-catalytic efficiency of building products.

References

[1] R. Benedix, F. Dehn, J. Quaas, M. Orgass, Application of titanium dioxide photocatalysis to create self-cleaning building materials, Lacer 5 (2000) 157–168.

[2] O. Carp, C.L. Huisman, A. Reller, Photoinduced reactivity of titanium dioxide, Progress in Solid State Chemistry 32 (2004) 33–177.

[3] J. Chen, S. Poon, Photocatalytic construction and building materials: from fundamentals to applications, Building and Environment 44 (2009) 1899–1906.

[4] I. Fasaki, K. Siamos, M. Arin, P. Lommens, I.Van Driessche, S.C. Hopkins, B.A. Glowacki, I. Arabatzis, Ultrasound assisted preparation of stable water-based nanocrystalline TiO_2 suspensions for photocatalytic applications of inkjet-printed films, Applied Catalysis A—General 411 (2012) 60–69.

[5] M. Shimohigoshi, Y. Saeki, Research and Application of Photocatalyst Tiles, Proceedings of the International RILEM Symposium on Photocatalysis, Environment and Construction Materials, Edited by P.Baglioni, L.Cassar and Florence, 2007, 291–297.

[6] P. Sao Marco, J. Marto, T. Trindade, J.A. Labrincha, Screen-printing of TiO_2 photocatalytic layers on glazed ceramic tiles, Journal of Photochemistry and Photobiology A: Chemistry 197 (2008) 125–131.

[7] D.M. Tobaldi, A. Tucci, G. Camera-Roda, G. Baldi, L. Esposito, Photocatalytic activity for exposed building materials, Journal of the European Ceramic Society 28 (2008) 2645–2652.

[8] M. Fassier, N. Chouard, C.S. Peyratout, D.S. Smith, H. Riegler, D.G. Kurth, C. Ducroquetz, M.A. Brunneaux, Photocatalytic activity of oxide coating on fired clay substrate, Journal of the European Ceramic Society 29 (2009) 565–570.

[9] ISO 10678. Fine Ceramics (Advanced Ceramics, Advanced Technical Ceramics). Determination of Photocatalytic Activity of Surfaces in an Aqueous Medium by Degradation of Methylene Blue, 2010.

[10] ISO 10676. Fine Ceramics (Advanced Ceramics, Advanced Technical Ceramics) . Test Method for Water Purification Performance of Semiconducting Photocatalytic Materials by Measurement of Forming Ability of Active Oxygen, 2010.

[11] ISO 22197-1. Fine Ceramics (Advanced Ceramics, Advanced Technical Ceramics). Test Method for Air-Purification Performance of Semiconducting Photocatalytic Materials, Part 1. Removal of Nitric Oxide, 2007.

[12] ISO 22197-2. Fine Ceramics (Advanced Ceramics, Advanced Technical Ceramics). Test Method for Air-Purification Performance of Semiconducting Photocatalytic Materials, Part 2. Removal of Acetaldehyde, 2011.

[13] ISO 22197-3. Fine Ceramics (Advanced Ceramics, Advanced Technical Ceramics). Test Method for Air-Purification Performance of Semiconducting Photocatalytic Materials, Part 3. Removal of Toluene, 2011.

[14] ISO 27447, Fine Ceramics (Advanced Ceramics, Advanced Technical Ceramics). Test Method for Antibacterial Activity of Semiconducting Photocatalytic Materials, 2009.

[15] ISO 27448, Fine Ceramics (Advanced Ceramics, Advanced Technical Ceramics). Test Method for Self-cleaning Performance of Semiconducting Photocatalytic Materials. Measurement of Water Contact Angle, 2009.

[16] 〈http://www.cost540.com/〉.

[17] T. Marolt, A.S. Škapin, J. Bernard, P. Zivec, M. Gabrscek, Photocatalytic activity of anatase-containing facade coatings, Surface and Coatings Technology 206 (6) (2011) 1355–1361.

[18] U. Cernigoj, M. Kete, U. Lavrencic Stangar., Development of a fluorescence-based method for evaluation of self-cleaning properties of photocatalytic layers, Catalysis Today 151 (2010) 46–52.

[19] J. Tschirch, D. Bahnemann, M. Wark, J. Rathouský, A comparative study into the photocatalytic properties of thin mesoporous layers of TiO_2 with controlled mesoporosity, Journal of Photochemistry and Photobiology A: Chemistry 194 (2008) 181–188.

[20] J. Tschirch, R. Dillert, D. Bahnemann, B. Proft, A. Biedermann, B. Goer, Photodegradation of methylene blue in water, a standard method to determine the activity of photocatalytic coatings?, Research on Chemical Inter-mediates 34 (4) (2008) 381–392

[21] N. Xu, Z. Shi, Y. Fan, J. Dong, J. Shi, M.Z.C. Hu, Effects of the particle size of TiO_2 on photocatalytic degradation of methylene blue in aqueous suspensions, Industrial and Engineering Chemistry Research 38 (1999) 373–379.

[22] C.H. Kwon, H. Shin, J.H. Kima, W.S. Choi, K.H. Yoon, Degradation of methylene blue via photocatalysis of titanium dioxide, Materials Chemistry and Physics 86 (2004) 78–82.

[23] V. Petrovic, V. Ducman, S.D. Skapin, Determination of the photocatalytic efficiency of TiO_2 coatings on ceramic tiles by monitoring the photodegradation of organic dyes, Ceramics International 38 (2) (2012) 1611–1616.

[24] L. Andronic, A. Enesca, C. Vladuta, A. Duta, Photocatalytic activity of cadmium doped TiO_2 films for photocatalytic degradation of dyes, Chemical Engineering Journal 152 (2009) 64–71.

[25] T. Ohsaka, F. Izumi, Y. Fujiki, Raman Spectrum of Anatase, TiO_2, Journal of Raman Spectroscopy 7 (6) (1978) 321–324.

[26] S.J. Rigby, A.H.R. Al-Obaidi, Soo-Keun Lee, D. McStay, P.K.J. Robertson, The application of Raman and anti-stokes Raman spectroscopy for in situ monitoring of structural changes in laser irradiated titanium dioxide materials, Applied Surface Science 252 (2006) 7948–7952.

[27] S. Stefanov, S. Batschwarov, Keramik Glasuren—Ceramic Glazes, Bauverlag GmbH, Wiesbaden und Berlin, 1988.

[28] A. Gucsik, M. Zhang, C. Koeberl, E.K.H. Salje, S.A.T. Redfern, J.M. Pruneda, Infrared and Raman spectra of $ZrSiO_4$ experimentally shocked at high pressures, Mineralogical Magazine 68 (5) (2004) 801–811.

[29] J. Winkler, Titanium Dioxide, Vincentz (European Coatings Literature), Hannover, 2003.

[30] D.M. Tobaldi, A. Tucci, A.S. Škapin, L. Esposito, Effects of SiO_2 addition on TiO_2 crystal structure and photocatalytic activity, Journal of European Ceramic Society 30 (12) (2010) 2481–2490.